European Journal of Neuroscience, Vol. 25, pp. 3526–3536, 2007 doi:10.1111/j.1460-9568.2007.05609.x

Exposure to retinoic acid at the onset of hindbrain segmentation induces episodic breathing in mice

Laura Guimarães,[1,2,*,‡] Eduardo Domínguez-del-Toro,[1,3,‡] Fabrice Chatonnet,[1,†,‡] Ludovic Wrobel,[1] Cristina Pujades,[4] Luís S. Monteiro[2] and Jean Champagnat[1]
[1]Neurobiologie Génétique et Intégrative, UPR 2216, CNRS, Gif-sur-Yvette, France
[2]Dept. Estudos de Populações, Instituto Ciências Biomédicas Abel Salazar, Porto, Portugal
[3]División de Neurociencias, Universidad Pablo de Olavide, Ctra. de Utrera, Km 1, Sevilla 41013, Spain
[4]Developmental Biology Group, Departament de Ciencies Experimentals i de la Salut, Universitat Pompeu Fabra, Barcelona, Spain

Keywords: Cheyne-Stokes breathing, Joubert syndrome, respiratory activity, rhombencephalon, rhythm generation

Abstract

Hyperpnoeic episodic breathing (HEB), a cyclic waxing and waning of breathing, has been widely reported in pre-term neonates, patients with Joubert syndrome and adults (Cheyne-Stokes respiration) with congestive heart failure and brainstem infarction. We now provide a developmental mouse model of neonatal HEB. We used retinoic acid (RA) (0.5–10 mg/kg of maternal weight) to alter embryonic development of the respiratory neuronal network at the onset of hindbrain segmentation (7.5 days post-coitum). HEB was observed *in vivo* after RA treatment during post-natal days 1–7 but not in control animals. HEB persisted after reduction of the chemoafferent input by hypocapnic hyperoxia (100% O_2). A large increase and decrease of the rhythm resembling an HEB episode was induced *in vitro* by stimulating the parafacial respiratory oscillator in treated but not in control neonates. Post-natal localization of the superior cerebellar peduncle and adjacent dorsal tegmentum was found to be abnormal in the pons of RA-treated juvenile mice. Thus, early developmental specifications in the rostral hindbrain are required for the development of neurones that stabilize the function of the respiratory rhythm generator, thereby preventing HEB during post-natal maturation.

Introduction

In mice, the embryonic stage during which the hindbrain is segmented is crucial for the development of brainstem neural networks regulating breathing. Anomalies of the respiratory rhythm have been described after inactivation of transcription factors with rhombomere (r) restricted expression patterns (reviewed by Lumsden & Krumlauf, 1996), e.g. *Hoxa1* with rostral expression matching the r3/r4 border or *Krox20* expressed in r3 and r5 (Jacquin *et al.*, 1996; Domínguez del Toro *et al.*, 2001; Chatonnet *et al.*, 2003b). The $Krox20^{-/-}$ and $Hoxa1^{-/-}$ mutations eliminate the r3r4-derived para-facial respiratory group (pFRG), an antiapnoeic neuronal system, that may exert a rhythm-promoting function on the more caudal pre-Bötzinger complex (pre-BötC) (Chatonnet *et al.*, 2003b) in the first few days after birth. The pre-BötC, derived from post-otic (r6r7) rhombomeres (Borday *et al.*, 2006), is a neuronal cluster within the ventrolateral medulla that is essential for maintaining respiratory rhythmogenesis (reviewed by Feldman & Del Negro, 2006). In contrast, nothing is known about the early embryonic events conditioning development of the rostral pontine control of breathing (reviewed in McCrimmon *et al.*, 2004).

Gain-of-function experiments suggest that segmental signalling at end-segmental stages [embryonic day (E)9.5 in mice, Giudicelli *et al.*, 2001] is sufficient to induce the development of rhythm generators (Coutinho *et al.*, 2004; Borday *et al.*, 2006). However, segmentation of the hindbrain starts at around E7.5 in mice (Lumsden & Krumlauf, 1996), the late streak stage, during which segmental expression of homeobox genes depends, amongst other controls, on a caudal-to-rostral endogenous gradient of retinoic acid (RA) (Gavalas, 2002; Maden, 2002). To investigate the importance of the late streak stage for breathing behaviour, we performed RA treatment at E7.5 in mice. This procedure is known to affect the spread of *Hox* and *Gbx2* expression domains into the anterior hindbrain; this is followed by a retraction that leaves behind a posteriorized expression pattern (Conlon & Rossant, 1992; Li & Joyner, 2001; Gavalas, 2002; Maden, 2002). We used sub-teratogenic doses of RA known to affect hindbrain segmentation (Pasqualetti *et al.*, 2001; Mic *et al.*, 2003; Sirbu *et al.*, 2005) and to allow post-natal survival. We found that doses as low as 0.5 mg/kg induce a behavioural phenotype including hyperpnoeic episodic breathing (HEB), a ventilatory instability reflecting an imbalance of central respiratory control (Han *et al.*, 2002).

Materials and methods

Mice

We used CD-1 mouse pups obtained by treating 14 pregnant females with an oral application of single all-*trans* RA doses ranging from 0.5

Correspondence: Dr Eduardo Domínguez del Toro, [3]División de Neurociencias, as above. E-mail: edomtor@upo.es

**Present address*: CIIMAR, Centro Interdisciplinar de Investigação Marinha e Ambiental, Laboratório de Ecotoxicologia, Rua dos Bragas 177, 4050-123 Porto, Portugal

†*Present address*: Institut de Génomique Fonctionelle de Lyon, UMR5242 CNRS/INRA/INSERM/École Normale Supérieure de Lyon, 46 allée d'Italie, 69364 Lyon Cedex 07, France

‡L.G., E.D.-d.-T. and F.C. contributed equally to this work.

Received 17 November 2006, revised 8 April 2007, accepted 30 April 2007

to 10 mg/kg of maternal bodyweight dissolved in dimethylsulphoxide and 0.2 mL of vegetable oil on E7.5 ('low-dose' group, $n = 11$ litters), with 0.05 mg/kg of maternal bodyweight on E7.5 ('very low-dose' group, $n = 3$ litters), and with 20 mg/kg of maternal body weight on E7.0 ('high-dose' group, $n = 3$ litters). Control females were administered the vehicle solution (dimethylsulphoxide and vegetable oil, without RA) at E7.5. The 12 h of the day of plug observation was considered as E0.5. Litter size, taken as an index of pre-natal survival, was similar for the control ($n = 6$ litters) and low-dose ($n = 11$ litters) groups. Neonates were apparently normal, with no mortality observed either at birth or during the time of analysis. In pilot experiments, no viable offspring were obtained from mice ($n = 3$) treated with 'very high doses' (20 mg/kg at E7.5), indicating foetal lethality, as previously reported (Conlon & Rossant, 1992; Marshall *et al.*, 1992). Such foetal lethality was not observed in the 'high-dose' group, which, however, exhibited significant post-natal mortality (30% compared with 2.7% in control mice, $P = 0.0002$ Fisher exact test). Electrophysiological and behavioural studies were carried out following the ethical guidelines of the European Union Council (86/609/EU), the French Agricultural Ministry and Spanish regulations (BOE 67/8509-12, 1988) for the care and use of laboratory animals in acute and chronic experiments. These experiments were also approved by the respective Institution Committees for animal care and handling.

Plethysmographic recording

Plethysmographic recordings concentrated on the first post-natal week during which previous studies on transgenic animals showed that crucial developmental stages take place for respiratory control (Jacquin *et al.*, 1996; Domínguez del Toro *et al.*, 2001). For each neonate we recorded over 10 [post-natal day (P)0–P6] samples (165 s) of the breathing behaviour, using a non-invasive barometric method previously described by Domínguez del Toro *et al.* (2001). Neonates were placed in a plethysmographic chamber (20 mL) kept at 31 °C, which was hermetically closed and connected to a differential pressure transducer (Validyne DP 103-14), a sine wave carrier demodulator (Validyne CD15) and a reference chamber. The plethysmographic signal was considered to reflect volume so that the contribution of gas rarefaction and compression might have distorted absolute values of tidal volume (V_T) in the smallest animals (Mitzner & Tankersley, 1998; Mortola & Frappel, 1998). This uncertainty was not further examined because similar effects of RA treatment on V_T are found using direct and barometric plethysmography and at different ages. A computer-assisted method was used to measure V_T, duration of inspirations (T_i) and expirations (T_e), and respiratory frequency (f). V_T was normalized with the body mass. Instantaneous minute ventilation (V_E) was calculated as $V_T \times f$. Instantaneous f, V_T and V_E were analysed for individual respiratory cycles of HEB episodes. Plethysmographic recordings were sub-divided into four patterns: HEB, non-HEB quiet breathing (breathing periods lacking hypernoeic episodes for more than 30 s), movements (during which respiratory pattern cannot be recorded) and apnoeas (expirations lasting longer than three respiratory cycles). The time spent in each of the above classified patterns was expressed as a percentage of the total recording time. Apnoeas and HEB are commonly present at birth, continuously decreasing throughout P0 to less than 2% of the total time. Average values of f, V_T and V_E in individual recordings were measured from periods of non-HEB quiet breathing and were expressed as a percentage of each HEB episode in order to evaluate evolutionary changes in respiratory pattern during the HEB episodes.

Hyperoxic tests were performed at P7 using direct plethysmography. The head of the animal was isolated from the rest of the body by a thin membrane that divided the recording chamber into two compartments of 20 mL each. The compartment containing the body was the recording chamber. The compartment containing the head was flushed at a rate of 0.3 L/min with humidified air (normoxic) or 100% O_2 (hyperoxic hypocapnic) gas for 40 s. This flow rate had no visible effect on the animal's behaviour. Given the flow rate and the volume of the chamber, the calculated time constant for filling the chamber was 3 s. At the end of the period of hyperoxia, the chamber was flushed with normoxic gas allowing the animal to recover eupnoeic breathing.

Isolated brainstem–spinal cord preparations

To investigate mechanisms of rhythm generation, we isolated brainstem–spinal cord preparations from 20 mice deeply anaesthetized with ether through a ponto-mesencephalic section (Fig. 4A) and a caudal section between cervical and thoracic rootlets. *In-vitro* recording was performed during P1 to be comparable to similar experiments performed on transgenic animals in which rhythm generation is affected (Borday *et al.*, 1997; Domínguez del Toro *et al.*, 2001; Chatonnet *et al.*, 2002). The preparation was pinned down with the ventral surface upwards in a 2 mL chamber bathed with artificial cerebrospinal fluid solution (pH 7.4) containing (in mM): 130 NaCl, 5.4 KCl, 0.8 KH_2PO_4, 26 $NaHCO_3$, 30 glucose, 1 $MgCl_2$ and 0.8 $CaCl_2$, saturated with carbogen (90% O_2, 10% CO_2) at 26–28 °C and perfused at a rate of 1–2 mL/min. Rhythm was recorded from hypoglossal rootlets. Data were stored on a PC using an interface (Labmaster) operating at a sampling frequency of 1 kHz. Smooth integration (Neurolog System) was performed from a full wave rectified signal with a 20 ms time constant.

To investigate the sensitivity of rhythm generators to afferent excitation, a stimulation of the rostral pole of the pFRG was performed by applying the glutamatergic agonist α-amino-3-hydroxy-5-methyl-4-isoxazoleproprionic acid (AMPA) (0.5 mM in artificial cerebrospinal fluid solution) and artificial cerebrospinal fluid solution alone below the ventral surface using a pressure pulse of 125 ms. Glass electrodes with a tip broken to about 5 μm and containing AMPA were located under the visual guidance of a microscope (ACM, Zeiss). The electrode was located in the rostral pole of the pFRG but we cannot exclude that AMPA had diffused more caudally to other respiratory control areas such as the retrotrapezoid nucleus or the pre-BötC. Previous experiments in similar conditions have shown that responses are abolished by moving the electrode by less than 400 μm (Domínguez del Toro *et al.*, 2001); no attempt was made to stimulate more caudal respiratory-related structures.

Pontobulbar sections (in Fig. 4A) were made at the level of the inferior cerebellar arteries in order to analyse the function of the bulbar rhythm generator, the pre-BötC, after isolation from the more rostral pFRG and A5 catecholaminergic control (see Chatonnet *et al.*, 2002). Rostral and caudal parts of the ponto-bulbar transections were placed in fixative, cut and stained with cresyl violet to identify the anatomical extent of isolated fragments.

Anatomical observation and immunochemistry

Mice were anaesthetized with pentobarbital (i.p.), and intracardially perfused for 15 min with 0.1 M phosphate-buffered saline (pH 7.4), followed by a mixture of 4% paraformaldehyde and 0.1% glutaraldehyde in 0.1 M phosphate-buffered saline. The brain was removed,

placed overnight in the same fixative and then rinsed in 0.1 M phosphate-buffered saline containing 15% sucrose and stored at 4 °C until used. Serial coronal, horizontal or parasagittal 40 μm sections were cut on a freezing microtome. Sets of four adjacent sections were processed using cresyl violet and polyclonal antibodies to tyrosine hydroxylase, choline acetyltransferase or acetylcholinesterase, as previously described (Domínguez del Toro *et al.*, 2001; Chatonnet *et al.*, 2002). The hindbrain/midbrain limit (see Fig. 6) was located between the retrorubral field (A8 midbrain group) expressing tyrosine hydroxylase and the adjacent pedunculo-pontine tegmental (PPTg) nucleus expressing choline acetyltransferase. The boundary between the tyrosine hydroxylase-expressing locus coeruleus (A6 r1-derived group) and the adjacent vestibular nuclei was considered the caudal limit of r1 (see Fig. 6B).

Anatomical defects were investigated in brainstem parasagittal sections as previously in *Krox20*, *Hoxa1* and *kreisler* homozygous mutants (Domínguez del Toro *et al.*, 2001; Chatonnet *et al.*, 2002) at a comparable post-natal age (P15–P20). Measurements in RA-treated animals are expressed as a percentage of the average values measured in controls (see locations in Fig. 7). The diameter of labelled structures was considered as the largest distance between stained cells. Distances between structures are measured at the medio-dorsal level where these structures are the largest. In the caudal brainstem, we measured the antero-posterior length of the ventral and dorsal pons between the pontine nuclei and the inferior olive, and between the anterior fourth ventricle diverticulum and the hypoglossal nucleus, providing the r4–r6-related index dorsal/ventral pons (see Domínguez del Toro *et al.*, 2001) as well as the distance between caudal limits of the nucleus ambiguus pars compacta and the facial nucleus (Amb, an r5-related index, see Chatonnet *et al.*, 2002). More rostrally, we measured the largest diameter of the facial nucleus (Mo7 r4-related, see Domínguez del Toro *et al.*, 2001), trigeminal (Mo5 r2r3-related) and pontine (r2r6-related) nuclei (see Jacquin *et al.*, 1996) as well as the distance between the trigeminal and facial nuclei (5–7d r3r5-related, see Jacquin *et al.*, 1996 and Chatonnet *et al.*, 2002). In the most rostral pons we also measured the length of the PPTg nucleus along its dorsocaudal–ventrorostral axis (the largest distance between PPTg neurones stained by choline acetyltransferase) and the length of the medial parabrachial nucleus along the dorso-ventral axis (estimated as the distance between the trigeminal/supra-trigeminal nucleus and the superior cervical peduncle). The abducens nucleus (Mo6), a structure eliminated by the *Krox20*, *Hoxa1* and *kreisler* homozygous mutations (see Chatonnet *et al.*, 2002), was also investigated by visually counting motorneurones exhibiting a visible nucleus from choline acetyltransferase-stained sections. All medio-lateral parts of the brainstem are taken into account in these measurements, including lateral (PPTg, medial parabrachial nucleus, Mo5, Mo7, Amb and 5–7d) and medial [Mo6, ventral pons (vP), and dorsal pons (dP)] structures. Measurements from mutants are published data except the most rostral measurements (locus coeruleus–retrorubral field, lateral parabrachial nucleus, medial parabrachial nucleus and PPTg), which were performed from original *Hoxa1*$^{-/-}$ and *kr*/kr sections.

Whole-mount in-situ *hybridization in embryos*

In situ hybridization was performed at E9.5, the stage at which segmental genes are expressed (and previously studied, see Dominguez del Toro *et al.*, 2001). Embryos were obtained from pregnant mothers killed by cervical dislocation according to the animal experimentation ethical committee. *In situ* hybridization was done using digoxigenin-labeled riboprobes as described by Wilkinson & Nieto (1993). Digoxigenin was detected with 4-Nitroblue tetrazolium chloride/5-Bromo-4-chloro-3-indolyl-phosphate (NBT/BCIP, Roche) which gives a purple staining. The riboprobes were as follows: *MafB/kreisler*, *Krox20*, *Hoxb1*, *Hoxb2*, *Hoxa2*, *Hoxa3*, *EphA4*.

Statistical analysis

All values are reported as means ± SEM. Correlation between birth weight and litter size was assessed by Pearson's product moment coefficient. Respiratory parameters and neurobehavioural performance were analysed by repeated-measures ANOVA or MANOVA, to test for the effect of treatment, followed by Scheffé's multiple comparison procedure. For the allometric study of V_T, an equation was computed for each animal relating V_T to body mass (M) from the daily values obtained during the first post-natal week. Exponents (b) and intercepts (a) relating the variables were derived from the linear least-squares regression analysis of the log-transformed equation $V_T = aM^b$. To test for the effect of treatment, the estimated exponents were taken as the dependent variable in a least squares analysis (Searle, 1971) using birth weight as a covariate. A Wilcoxon test for matched pairs was used to assess differences in respiratory parameters after hyperoxia and in hindbrain rhythmic activity *in vitro* before and after AMPA stimulation, as well as after ponto-bulbar sections. Statistical significance was accepted for $P < 0.05$. Statistical procedures were carried out on LSMLMW (Harvey, 1985) and SPSS 13.0.

Results

Abnormal respiratory pattern in retinoic acid-treated mice

Hyperpnoeic episodic breathing episodes were defined as transient hyperventilations (400% increase of V_E) lasting for 10–20 s so that episodes occurring at a frequency of 3/min or more revealed a periodic HEB pattern (bottom trace in Fig. 1A). Samples lacking episodes for more than 30 s (top trace in Fig. 1A) revealed non-HEB quiet breathing patterns. Figure 1B shows the average time course of HEB episodes recorded at the end of the first post-natal week (seventh post-natal day, P6) in mice treated with low doses of RA. HEB episodes started and terminated gradually, with waxing and waning of respiratory amplitude (V_T) and frequency (f) (Fig. 1, B2). At the end of HEB episodes, V_E (minute volume, $V_E = V_T * f$) was weak (Fig. 1, B1) but no apnoea was observed. In contrast to RA-treated animals, controls exhibited exclusively non-HEB breathing, with oscillations of V_E that never exceeded 20% of average values ('Control' in Fig. 1B).

The occurrence of HEB was related to pre-natal RA administration in a dose-dependent manner. The 0.05 mg/kg dose was ineffective (Fig. 1, C1). HEB episodes were increased in mice treated with 0.5–10 mg/kg. During non-HEB quiet breathing, 71% of treated mice (0.5–10 mg/kg) also retained low values of V_T (Fig. 1, C2) as well as large variability of the expiratory time (coefficient of variation, 50% in treated mice vs. 21% in controls). Irregularity of the rhythm, scored from the average difference in duration of successive cycles ($n = 100$ per animal, see Telgkamp *et al.*, 2002), was larger in RA-treated mice (37.6 ± 15.9 ms, $n = 11$) than in controls (9.0 ± 2.1 ms, $n = 14$).

Post-natal maturation of breathing

The occurrence of HEB was measured every day during the first week in mice treated with 0.5–10 mg/kg RA. HEB emerged during the second post-natal day (P1) and persisted during the first post-natal week in 64% of RA-treated animals. HEB duration was significantly

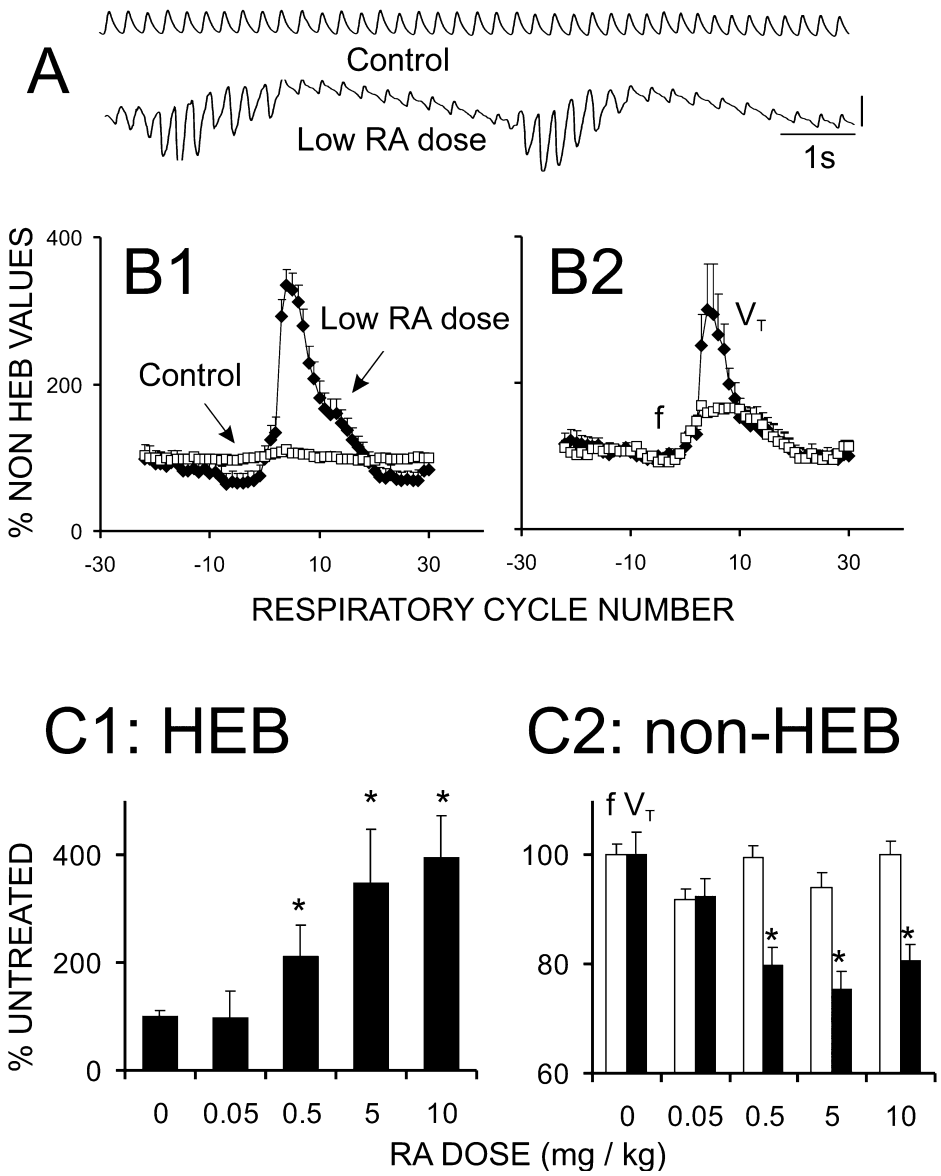

FIG. 1. Breathing pattern at post-natal day (P)6 following treatment with low doses of retinoic acid (RA). (A) Plethysmographic recordings of non-hyperpnoeic episodic breathing (HEB) quiet breathing in a control pup (top trace) and periodic HEB in RA-treated animal (calibrations 1 s, 50 μL). (B) Minute volume (V_E) (B1), respiratory frequency (f) and tidal volume (V_T) (B2) during HEB episodes at P6 in low-dose RA-treated mice ($n = 10$; mean ± SEM); small oscillations of V_E during non-HEB breathing in controls ($n = 14$, B1) are presented for comparison; parameters are expressed as a percentage of non-HEB value in each animal. (C) Frequency of HEB episodes (C1), respiratory frequency (f) and tidal volume (V_T) during non-HEB quiet breathing (C2, ± SEM, $^*P < 0.05$) induced at P6 after different doses of RA: 0 (controls), $n = 37$; 0.05 mg/kg, $n = 13$; 0.5 mg/kg, $n = 24$; 5 mg/kg, $n = 13$; 10 mg/kg, $n = 14$. Note the dose-dependency of effects on HEB appearance and quiet breathing reduction of V_T.

longer than in controls at P1 (Table 1) and progressively increased during the first 5 days (Fig. 2A). The same result was seen in the high-dose group (Table 1).

To investigate non-HEB breathing during the same post-natal period, we studied the allometric relationship between respiratory amplitude (V_T) and body mass (M). We computed for each pup (normal and low-dose RA-treated mice) the equation of V_T as a function of M ($V_T = aM^b$; see Statistical Analysis) derived from the least-squares regression fitted to the daily values between birth and P6. We also considered how the size of each individual at birth influenced the rate of increase of V_T, by taking exponents b as the dependent variable in a least squares analysis (Searle, 1971), using birth weight as a covariate. Values of b larger or smaller than unity indicate that V_T varies at a rate that is, respectively, disproportionately greater or smaller than M. We found that RA treatment at low doses disrupted the relationship between V_T and M and that this effect was significantly influenced by the animals' weight at birth ($b = 1.11 \pm 0.24$, $R^2 = 0.46$, $P < 0.001$ for the low-dose group compared with $b = -1.09 \pm 0.029$, $R^2 = 0.34$, $P < 0.001$ for controls, Fig. 2B). In controls, the increase of V_T per unit change of M was higher in smaller neonates. Thus, after RA treatment, V_T was not only small in the population of treated animals but it also increased at a slower rate than normal, particularly in smaller neonates, which seemed unable to provide a V_T adequate to their size.

Therefore, RA administration causes non-HEB respiratory abnormalities as well as HEB during the first post-natal week. Treated mice at P1 were also hyperactive (moving during 17% of the time vs. 3% in controls), with a faster than normal righting reflex and relatively weak

TABLE 1. Respiratory and behavioural parameters in controls and low- and high-dose groups at post-natal day 0.5–P1.5

	Controls ($n = 31$)	Low-dose group ($n = 57$)	High-dose group ($n = 17$)
Litter size	13 ± 1.94	11 ± 0.79	10 ± 1.53
Birth weight (g)	1.48 ± 0.032	1.47 ± 0.026	1.55 ± 0.044
V_E (mL/g/min)	1.21 ± 0.08	1.07 ± 0.05	0.82 ± 0.02**
Apnoeas (%)†	2.1 ± 0.53	2 ± 1.02	1.4 ± 0.83
HEB (%)†	0.2 ± 0.2	4.6 ± 1.3***	8.5 ± 1.5***
Suction (*n* per 30 s)‡	35 ± 1.04	26 ± 1.12***	28 ± 1.52***
Motility (%)†	3.2 ± 1.11	17.4 ± 2.97***	30.7 ± 4.46***
Righting (s)§	13 ± 1.02	7 ± 0.75***	8 ± 1.03**

V_E, non-hyperpnoeic episodic breathing (HEB) respiratory minute volume. †Percentage of the total time of plethysmographic recording. ‡Suction activity was evaluated by counting the number (per 30 s) of jaw openings elicited by a peribuccal contact; motility corresponded to the duration of limb, neck or body movements in the plethysmographic chamber. §The righting reflex was assessed as the time (s) the animal took to roll over when placed on its back. ***$P < 0.001$, **$P < 0.01$ compared with control values.

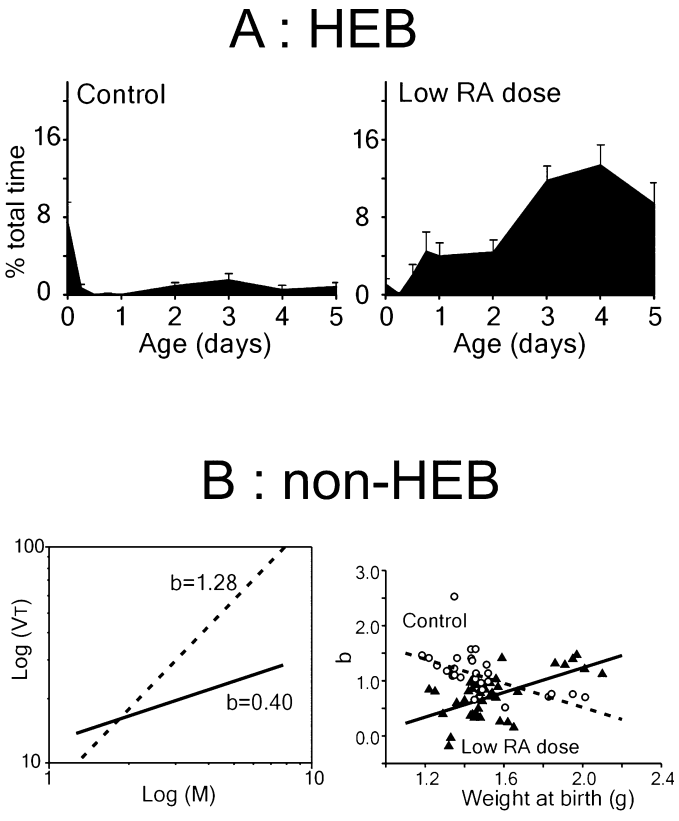

FIG. 2. Evolution of hyperpnoeic episodic breathing (HEB) (A) and non-HEB (B) respiratory parameters during the first post-natal week. (A) Evolution of the duration of HEB from birth to post-natal day 5. (B) Retinoic acid (RA)-induced disruption of the allometric growth of tidal volume (V_T). Estimated 'b' exponents for individual mice (μL/g, ordinate) were taken in a least-squares analysis to test for the effect of RA; birth weight (BW) (g, abscissa) was used as a covariate to allow for the animal's early or retarded development at delivery (see Materials and methods). After low-dose RA there was an abnormal growth of V_T, which depended on BW. The slope of the b/BW relationship is negative (-1.09 ± 0.29 μL/g^2) for the control group (open circles, dashed line) and positive ($+1.11 \pm 0.24$ μL/g^2) for the treated group (black triangles, continuous line). Low-BW (1.2–1.5 g) treated neonates exhibit changes in V_T at a rate lower than body mass (M) in contrast to low-BW control mice.

suction activity (Table 1). These observations indicate that, in RA-treated mice, HEB is part of a behavioural phenotype affecting the control of respiratory depth and brainstem-controlled motor activities as early as P1.

Effect of hyperoxia on the breathing pattern

Hyperpnoeic episodic breathing in rodents is affected by the activity of chemoreceptors (Han *et al.*, 2002). We thus investigated involvement of the chemosensitivity in the generation of HEB at P7. In 14 low-dose-treated mice, HEB and non-HEB patterns were analysed before and during a short exposure to hypocapnic hyperoxia, in order to minimize on-going O_2-sensitive respiratory drive as well as stimulation by CO_2. Hyperoxia did not eliminate or reduce the RA-induced HEB, indicating that HEB generation requires central circuits rather than peripheral chemoreceptors. In fact, during hyperoxia, HEB episodes were significantly increased in frequency and followed by long expirations or apnoeas (Fig. 3) in nine out of 14 animals, indicating that chemoreflexes tend to stabilize breathing. HEB was unchanged in the remaining five tested animals. During non-HEB quiet breathing, the minute ventilation was decreased by hyperoxia to 70.8 ± 3.67% of normoxic values. The frequency and amplitude of breathing were decreased, this effect being the same in control and treated animals, indicating a normal efficacy of the chemoreflex control in RA-treated mice.

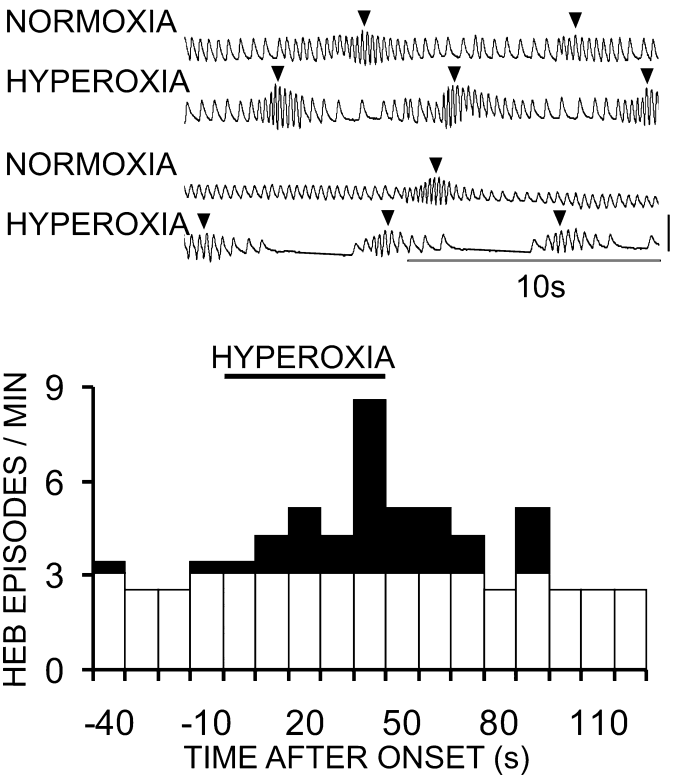

FIG. 3. Effect of hyperoxia on the retinoic acid-induced hyperpnoeic episodic breathing (HEB) at post-natal day 7. Top: plethysmographic samples from two different animals in normoxia and hyperoxia; arrowheads indicate HEB episodes. Note slow frequency (animal on top) and apnoeas during hyperoxia. Bottom: average ($n = 14$) frequency of HEB episodes during hyperoxic tests. Hyperoxia (bar above histogram; onset is time 0 on abscissa) increases the frequency of HEB episodes (min^{-1}, ordinate).

Respiratory rhythm generation in the brainstem isolated in vitro

We investigated brainstem respiratory rhythm generation after RA treatment in both the low- and high-dose groups. We used a brainstem–spinal cord preparation isolated *in vitro* at P1 (Fig. 4A).

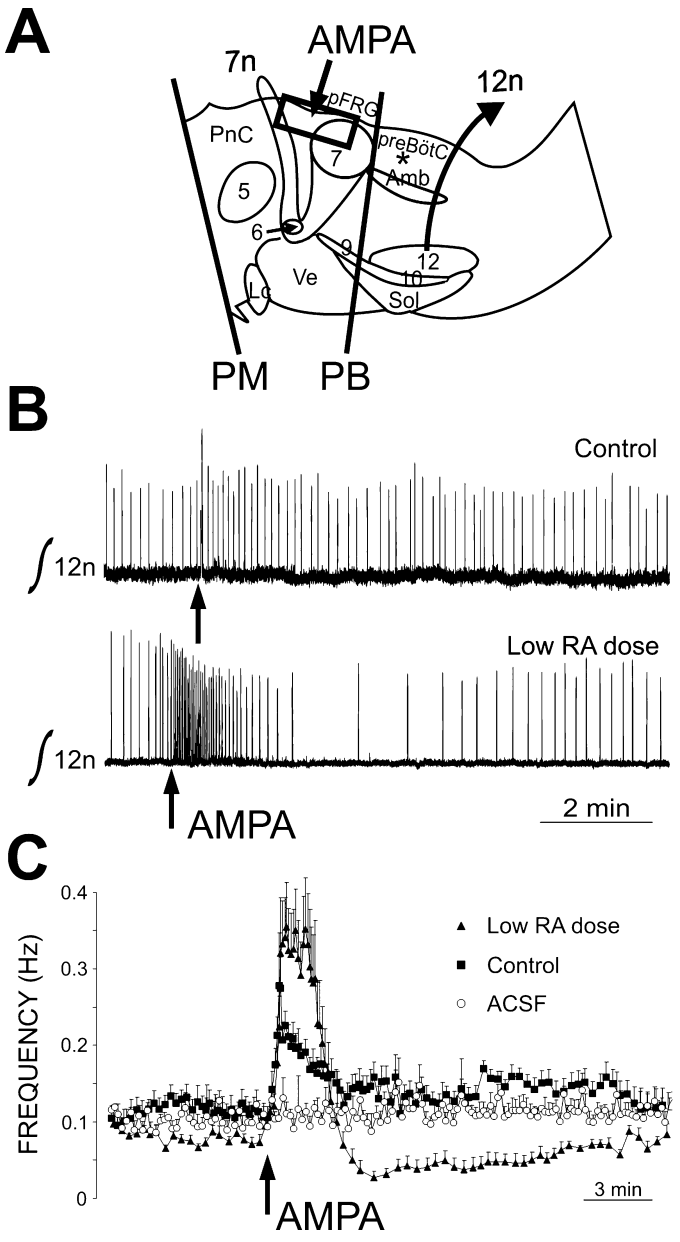

FIG. 4. Rhythm generation *in vitro* at post-natal day 1 in retinoic acid (RA)-treated mice. Rhythmic activity generated by control and RA-treated isolated brainstem–spinal preparations. (A) Schematic presentation. The approximate antero-posterior extension of α-amino-3-hydroxy-5-methyl-4-isoxazolepropri-onic acid (AMPA)-induced stimulation (rectangle, estimated from Domínguez del Toro *et al.*, 2001) indicates that the para-facial respiratory group (pFRG) and A5 are stimulated, although diffusion of AMPA to the pre-Bötzinger complex (pre-BötC, *) cannot be entirely excluded. PM, ponto-mesencephalic; PB, pontobulbar sections; AMPA, location of pressure application; 5–10, cranial motor nuclei; 12n, recorded hypoglossal nerve; Amb, nucleus ambiguus; Ve, vestibular nucleus; Sol, solitary complex; Lc, locus coeruleus; PnC, caudal pontine nuclei. (B) Integrated nerve recordings during a pressure (125 ms) AMPA application. An upward deflection indicates a burst of motor activity. (C) Average (± SEM) changes in rhythm frequency induced by AMPA [0.5 mM in artificial cerebrospinal fluid solution (ACSF)] in control ($n = 7$) and low-dose ($n = 5$) groups, as well as ACSF in control group ($n = 8$).

This preparation retains the activity of the dual respiratory oscillator comprising the pre-BötC caudally and the pFRG rostrally. The frequency of the rhythm (see recordings before stimulation in Fig. 4B and C) was similar in untreated controls (0.09 ± 0.009 Hz, $n = 10$) and in the low-dose group (0.10 ± 0.03 Hz, $n = 10$), whereas the rhythm was depressed ($P < 0.05$) in the high-dose group (0017 ± 0.003 Hz, $n = 10$).

The responsiveness of the rhythm generators to afferent excitation was tested using pressure applications of the glutamatergic agonist AMPA in the area of the pFRG, caudal to the exit point of the facial nerve. Stimulation with AMPA increased the rhythm frequency in both control and treated mice, in keeping with the rhythm-promoting function of the pFRG. However, after treatment with low doses of RA, AMPA induced additional responses that were not seen in controls; an episode comprising 10–20 respiratory bursts was elicited and followed by a period of apnoea ($n = 5$, Fig. 4B and C, frequency increased by 0.1 Hz in control and 0.25 Hz in low-dose RA). It seems therefore that, in these mice, the rhythm generator is hyper-excitable by an excitatory input. Generators were also hyper-excitable after treatment with high doses of RA because a significant response was preserved despite the almost complete depression of the on-going rhythm generation in the high-dose RA animals (data not shown).

The function of the pre-BötC alone was recorded after transversal section of the brainstem at the caudal limit of the facial motor nucleus (pontobulbar section in Fig. 4A). In the low-dose RA-treated group, the rhythm of the isolated pre-BötC was the same as in controls (0.23 ± 0.02 Hz). However, the isolated pre-BötC was significantly slower ($P < 0.05$) in the high-dose group (0.12 ± 0.03 Hz, $n = 5$). By comparing frequencies measured before and after the section, we obtained an evaluation of the inhibitory control exerted by the A5 catecholaminergic cell group on the pre-BötC (see Chatonnet *et al.*, 2002). After the section, the frequency increased similarly (by about 0.12–0.13 Hz) in all groups, suggesting that the RA treatment does not impair the A5 inhibition.

Altogether, *in-vitro* experiments show that treatment with a low dose of RA does not disturb on-going rhythm generation but exaggerates the response of respiratory generators to afferent excitatory input.

Anatomical abnormalities

A consistent anatomical reorganization was observed in the rostral and dorsal pons of low-dose mice. Cholinergic neurones of the PPTg nucleus were spread ventrally and rostrally into a territory 22 ± 6% larger than in control mice so that the PPTg protruded into the midbrain domain (Fig. 5). Although the overall rostro-caudal extent of the r1-derived dorsal pons was not changed (as measured from the caudal limits of the retrorubral field rostrally to the locus coeruleus caudally, Fig. 5B), the cholinergic territory appeared to increase at the expense of adjacent ventral and caudal structures, including laterally the nucleus parabrachial medialis (reduced by 27 ± 3%, double arrow in Fig. 5A) and medially the A5 (SubC) catecholaminergic group (Fig. 5B). As a consequence, PPTg ectopic neurones expressing choline acetyltransferase were found in a ventral and rostral position where, in controls, the pontine oralis nucleus is non-cholinergic. This was associated with an abnormal orientation of the superior cerebellar peduncle (scp) in the vicinity of the PPTg (green cells in Figs 5 and 6A). In horizontal sections (Fig. 6A), the scp is orientated at a 45° angle with respect to the medial line (dotted line in Fig. 6A), whereas it runs more parallel to the midline in treated animals (arrow in Fig. 6A, right). As a consequence, in parasagittal sections at the

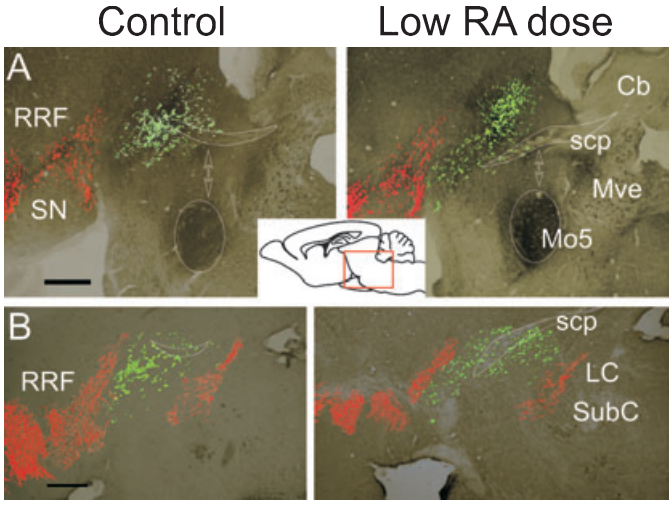

FIG. 5. Parasagittal views from three adjacent sections showing control (left) and retinoic acid (RA)-treated (right) rostral pontine structures (dorsally, top and ventrally, bottom). (A) View (dorsal is top and rostral is left) at the level of the parabrachial nucleus showing the choline acetyltransferase immunoreactivity of the rhombomere 1-derived pedunculo-pontine tegmental (PPTg) (green) and tyrosine hydroxylase immunoreactivity (red) of the retrorubral field (RRF) and substantia nigra (SN). Cholinesterase immunoreactivity (background) shows surrounding structures; the superior cerebellar peduncle (scp) and the trigeminal motor nucleus (Mo5) are outlined. Cb, cerebellum; MVe, medial vestibular nucleus. (B) Parasagittal section (medial to the plane illustrated in A, from different animals) showing the choline acetyltransferase immunoreactivity of the PPTg (green) and tyrosine hydroxylase immunoreactivity of the locus coeruleus (LC), SN and PPTg (red). SubC, subcoeruleus. Calibration bars, 500 μm.

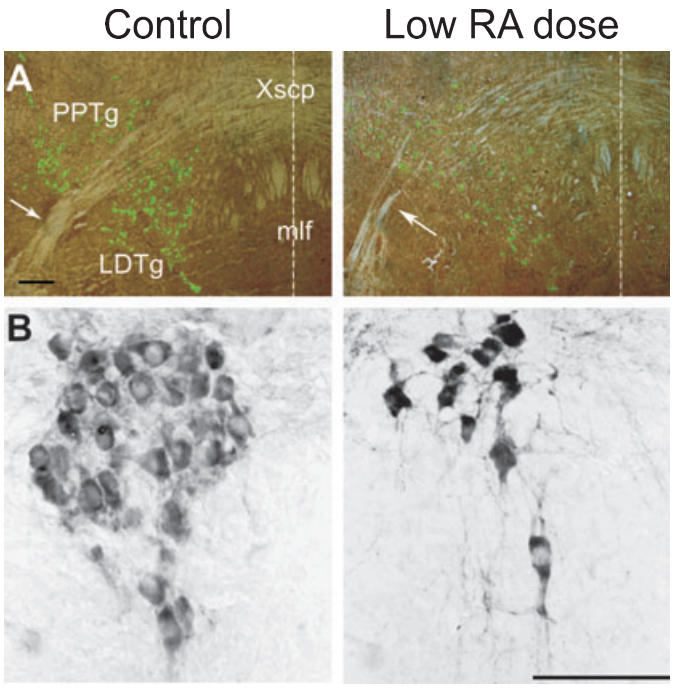

FIG. 6. Dorsal modifications affecting superior cerebellar peduncle and abducens nucleus. (A) Horizontal section stained by cholinesterase immunoreactivity showing displacement of the superior cerebellar peduncle (arrows) with respect to the medial line (dotted line on the right). LDTg, latero-dorsal tegmental nucleus; mlf, medial longitudinal fasciculus; Xscp, decussation of the superior cerebellar peduncle. (B) Parasagittal view of the abducens nucleus (Mo6), processed with an antibody against choline acetyltransferase at post-natal day 7, was hypoplasic in retinoic acid (RA)-treated mice. Calibration bars: 200 μm (A) and 100 μm (B). PPTg, pedunculo-pontine tegmental.

level of the trigeminal nucleus (Figs 5A and 7A) or locus coeruleus (Figs 5B and 7A), the scp is well orientated until it reaches the PPTg and then goes more rostral and ventral in treated animals than in control. The most caudal deficit was found in the abducens somatic motor nucleus (Fig. 6B), a structure eliminated by the mutation of many segmental genes (*Krox20*, *Hoxa1* and *MafB*/kreisler, see Chatonnet *et al.*, 2002) and exhibiting 52 ± 16% less motoneurones ($P < 0.001$) in RA-treated mice than in controls.

In contrast, the anatomy of the ventral pontobulbar structures and the segmental organization of branchiomotor nuclei were normal. The size and boundaries of rhombomeres in the r3–r5 territory were normal as assessed from the expression of *Hoxb1*, *Krox20*, *Hoxa2*, *Hoxb2*, *kreisler*/MafB and *EphA4* in the neural tube at E9.5 and E10.5 (data not shown) as previously reported for similar doses (Pasqualetti *et al.*, 2001). We also investigated anatomical deficits in caudal pontine and medullary parts of the brainstem and compared measurements in RA-treated animals with those observed in *Krox20*, *Hoxa1* and *kreisler* null-mutations, which eliminate r3-, r4- and/or r5-derived territories. We found a normal antero-posterior length of the dorsal and ventral pons (dP and vP in Fig. 7), and a normal position of the nucleus ambiguus and facial branchial motor nucleus (Amb in Fig. 7) in low-dose-treated mice, contrasting with abnormal values in *Hoxa1* and *kreisler* mutants. The parvocellular reticular nucleus, a dorsal pontine structure originating in r3 and extending between the trigeminal motor nucleus and facial nerve (Mo5–7 in Fig. 7), was normal. Pontine and trigeminal nuclei, reduced in *Krox20* mutants, and the facial nucleus, reduced in *Hoxa1* mutants, were also normal after RA treatment (pontine, Mo5 and Mo7 in Fig. 7). It seems therefore that major brainstem defects that might disturb the respiratory behaviour after treatment with low doses of RA are restricted to the dorsal and rostral pons.

Discussion

The present study identifies respiratory and anatomical abnormalities following the administration of sub-teratogenic doses of RA at the late streak stage of embryonic development. This provides pharmacological support for transgenic animal models demonstrating that disruption of the early genetic programme orchestrating hindbrain development causes aberrant anatomo-functional organization of the brainstem neuronal network controlling breathing after birth. The RA-induced respiratory deficit, HEB, is observed in mice in the absence of an obvious anomaly of the rhythm generators and is attributed to rostral pontine anomalies, as in the human Joubert syndrome.

Central generation of hyperpnoeic episodic breathing

Massive occurrence of HEB was the major post-natal respiratory defect induced by the administration of RA at E7.5. It is generally accepted that HEB reflects instability in the respiratory control system (Cherniack *et al.*, 1966; Khoo *et al.*, 1982; Bruce & Daubenspeck, 1995; Cherniack, 1999). Human and animal studies have provided evidence supporting the importance of hypoxia, altitude acclimatization and hypocapnia in the induction of HEB so that ventilatory instability may result from the unbalanced control of the rhythm generators by peripheral and central afferent controls (Han *et al.*, 2002; Topor *et al.*, 2006). We now show that HEB persists after the reduction of on-going chemosensory drive. This confirms the previous conclusion that genetically controlled HEB cannot be mediated by peripheral chemoreceptors only (Han *et al.*, 2002). The present results also support the idea that blockade of the peripheral chemoafferent

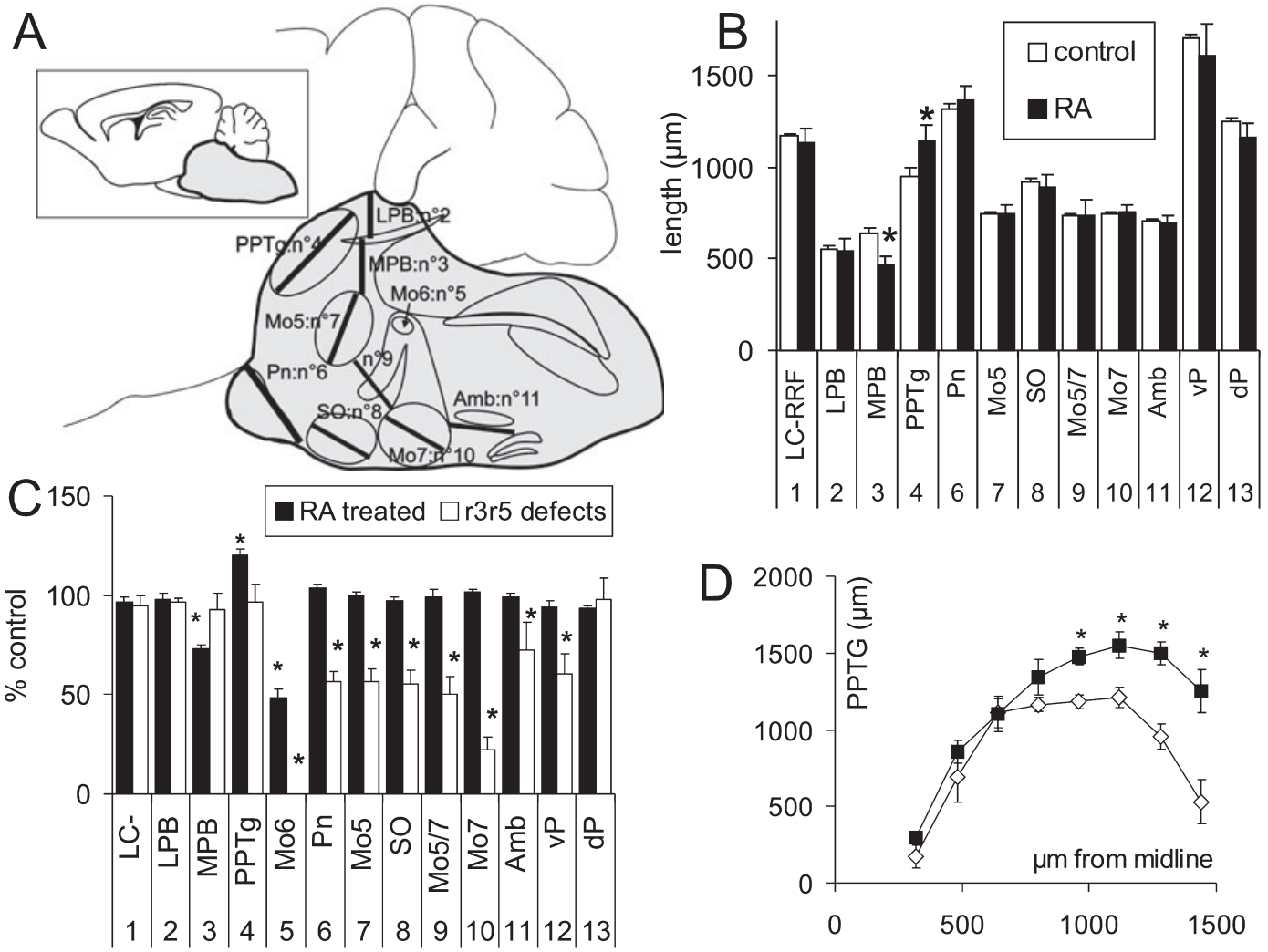

FIG. 7. Pontine abnormalities in retinoic acid (RA)-treated mice. (A) Schematic parasagittal view of the brainstem structures studied. (B) Histogram showing the length (µm) of brainstem structures after control (white bars, $n = 11$) and RA treatments [black bars, $n = 11$; see black bars in A, locus coeruleus–retrorubral field (LC–RRF) no. 1, ventral pons (vP) no. 12 and dorsal pons (dP) no. 13, not shown in A for clarity, are, respectively, between the caudal limits of LC and RRF (red cells in Fig. 5), caudal pontine (Pn) and rostral inferior oliva, rostral hypoglossal and abducens nuclei]. Significant changes (Mann–Whitney *U*-test, $*P < 0.01$) are only seen in no. 3–4. (C) Measurements as in A and B expressed as a percentage of control, comparing RA-treated mice and previously studied mutants with abnormal r3–r5 development: *kr*/kr (no. 11, $n = 4$, Chatonnet *et al.*, 2002), *Hoxa1*$^{-/-}$ (no. 10, 12–13, $n = 4$, Domínguez del Toro *et al.*, 2001) and *Krox20*$^{-/-}$ (no. 6–9, $n = 4$, Jacquin *et al.*, 1996). Measurements in *kr*/kr and *Hoxa1*$^{-/-}$ are averaged in no. 1–4. The abducens nucleus (no. 6) is absent in mutants. Note that no. 3–4 affected by RA (*) are normal in mutants, whereas no. 6–12 affected in mutants (*) are normal after RA treatment. (D) Length of the pedunculo-pontine tegmental nucleus (no. 4 in A–C, green cells in Fig. 5) in parasagittal sections at different medio-lateral levels from the midline; a significant increase (Mann–Whitney *U*-test, $*P < 0.01$) is found at lateral levels including the locus coeruleus (960–1120 µm, Fig. 6B) and trigeminal nucleus (1280–1440 µm, Fig. 6A). Amb, distance between caudal limit of Mo7 and pars semicompacta of the nucleus ambiguus; LPB, lateral parabrachial nucleus; MPB, medial parabrachial nucleus; Mo5, 6, 7, trigeminal, abducens, facial motor nuclei; SO, superior olive; Mo5/7, interval between Mo5 and Mo7; PPTg, pedunculo-pontine tegmental nucleus.

input by inhalation of a hyperoxic gas against a background of hypoxia promotes instability in the respiratory controller (Wilkinson *et al.*, 1997; Han *et al.*, 2002). We have found *in vivo* that oxygen administration exaggerates HEB and favours the association of HEB episodes with apnoeas in RA-treated mice. An even more dramatic instability including apnoea is found after maximal de-afferentation *in vitro* and parafacial stimulation with AMPA. It seems therefore that a variety of inputs controlling breathing during normoxia stabilizes the respiratory rhythm *in vivo* and that chemosensory inputs are not sufficient to explain the RA-induced HEB.

Mice treated with RA allowed the mechanisms responsible for HEB to be investigated *in vitro*. Large responses including apnoeas, induced by stimulating the pFRG with AMPA, revealed the instability of the respiratory rhythm generation. Recent results suggest that the respiratory rhythm is generated by two coupled oscillators, the pre-BötC and pFRG (reviewed by Feldman & Del Negro, 2006; see also Chatonnet *et al.*, 2003b). Such duplication may be a mechanism that reduces vulnerability by splitting the generator into distinct units, each with specific but cooperating functions. However, duplication also implies non-linear dynamic interactions between the two units that, once perturbed, may cause breathing instability according to mathematical simulation studies (see Bruce & Daubenspeck, 1995). A reduced activity of the pre-BötC probably complicates the HEB patterns and reduces respiratory frequency in animals treated with high RA doses. In contrast, on-going rhythm generation in the absence of AMPA stimulation *in vitro* indicates no abnormal function of the dual generator, pre-BötC alone and A5-related respiratory depression in low-dose-treated mice. Accordingly, low respiratory frequency and

neonatal apnoeas indicating dysfunction of the generator in other animal models *in vivo* (Domínguez del Toro *et al.*, 2001; Chatonnet *et al.*, 2003a) were not seen after RA treatments with low doses. We therefore consider that HEB is centrally generated but does not result exclusively from an abnormality of the rhythm-generating process alone.

Possible pontine control of hyperpnoeic episodic breathing

The RA treatment probably induces anomalies in the interactions between the rhythm generators and other respiratory-related brainstem structures. In fact, some aspects of the HEB pattern induced by RA were not preserved *in vitro*. In RA-treated animals *in vivo*, HEB episodes occur spontaneously, changing both V_T and frequency. In contrast, the burst amplitude *in vitro* was not consistently affected before or after AMPA stimulations. Therefore, afferent inputs that are inactive or eliminated *in vitro,* particularly the afferents from the rostral pons, are required to trigger a fully developed HEB pattern. The response obtained with AMPA *in vitro* suggests that the responsiveness of the respiratory generator to these excitatory inputs is abnormally high and probably sufficient *in vivo* to trigger HEB episodes. Complex central modulations and reflex adjustments may ensue *in vivo* to modulate V_T, stabilize the rhythm and prevent apnoeas after HEB episodes.

Altogether, the present study on HEB and previous studies on rhythm generators (Jacquin *et al.*, 1996; Domínguez del Toro *et al.*, 2001; Chatonnet *et al.*, 2002) suggest that developmentally distinct neuronal systems control the shaping of inspirations *in vivo*. Lumsden (1923) first suggested that the brainstem respiratory controller is organized along the antero-posterior axis up to a distinct rostral pontine respiratory group of neurones, later located in the medial parabrachial and Kölliker-Fuse nuclei (McCrimmon *et al.*, 2004; Kobayashi *et al.*, 2005; Potts *et al.*, 2005). It is tempting to speculate that HEB generation in the present study results from an abnormal interaction of these pontine neurones with the rhythm generators. However, RA treatment also affects other respiratory-related pontine structures, particularly the PPTg responsible for the cholinergic control of the generator. Impairment of this control by homozygous inactivation of the gene encoding the acetylcholinesterase enzyme induces an abnormal control of V_T in adult knock-out mice, whereas the rhythm generator adapts to hypercholinergy by decreasing the synaptic efficacy of nicotinic and muscarinic agonists (Chatonnet *et al.*, 2003a). Therefore, the RA-induced HEB may result from an abnormal interaction of the respiratory rhythm generators with pontine respiratory and/or cholinergic afferents.

Abnormal development at the onset of hindbrain segmentation causes aberrant anatomo-functional organization of the pons

Anatomical deficits in the rostral pons adjacent to the midbrain territory probably result from a direct posteriorizing effect of exogenous RA on the neural tube close to the midbrain/hindbrain boundary. Development of the rostral hindbrain requires the homeobox gene *Gbx2* that later demarcates the presumptive midbrain/hindbrain junction. Within 4 h of treatment at E7.5, RA has been shown to strongly up-regulate *Gbx2* and to expand its expression domain anteriorly (Li & Joyner, 2001). In addition, exogenous RA is expected to be particularly effective at this level of the neural tube where the endogenous RA activity is maintained low at E7.5 by the RA-degrading enzyme Cyp26a1 (Sirbu *et al.*, 2005). In contrast, in the more caudal hindbrain, large endogenous RA activity (Gavalas, 2002; Maden, 2002) probably limits the relative efficacy of low doses of exogenous RA at physiological targets. An alternative explanation for the RA-induced rostral pontine deficits would be that sufficient exogenous RA persists until E9.5–10.5, a stage at which RA is known to affect the neuronal migration of pontine nuclei (Yamamoto *et al.*, 2003) or neuronal phenotypes (Holzschuh *et al.*, 2003). We consider it unlikely that exogenous RA at doses 1–2 orders of magnitude lower than 20 mg/kg remains active on the hindbrain for several days. In pilot experiments using 20 mg/kg RA, we found that the lethal effect of administration at E7.5 was clearly alleviated by advancing administration to E7.0 ('high dose'), indicating that the activity of RA decreases significantly within 0.5 day. It has also been reported that the rostral shift of rhombomere boundaries induced by 5 mg/kg RA at E8 is seen at E8.5 but not any longer at E9.5 (Pasqualetti *et al.*, 2001). In the present study, respiratory frequency and lack of lethal apnoeas after RA treatment indicate that the development of the rhythm generators is normally induced at E9.5 and later (Coutinho *et al.*, 2004; Borday *et al.*, 2006) It is therefore unlikely that RA doses as low as 0.5 mg/kg administered at E7.5 remain active at end-segmental stages (E9.5). The present study rather suggests that respecification of progenitors by RA at early stages of hindbrain segmentation can effectively and irreversibly alter the fate of pontine neurones or axonal trajectories originating from r1–r2 (Oury *et al.*, 2006).

Inherited control of hyperpnoeic episodic breathing

As RA controls gene transcription, the present results suggest that HEB might be an indication of congenital abnormalities in the central respiratory control. The observation of HEB in young infants may be a sign of rostral pontine dysfunction indicating the need for careful examination of the anatomy and function of pontine-derived territories. Previous studies in mice support the idea that instability of breathing could be genetically inherited because HEB could be induced in C57BL/6J but not in A/J strains during reoxygenation after hypoxia (Han *et al.*, 2002). Genes operating during early pontine development may therefore be involved in changing susceptibility to HEB.

The respiratory and anatomical anomalies of RA-treated mice resemble several traits reported in human pathologies such as the Joubert syndrome. This is a genetically heterogeneous syndrome with three known loci, 9q34.3 (JBTS1), 11p11-q12 (CORS2/JBTS2, Lagier-Tourenne *et al.*, 2004) and JBTS3, on chromosome 6q23.2-q23.3 (Ferland *et al.*, 2004). It is also clinically heterogeneous with breathing abnormalities including HEB (in 60–80% of patients) in the neonatal period, oculomotor apraxia (in 75% of patients), ataxia and mental retardation (Joubert *et al.*, 1969; Saraiva & Baraitser, 1992; Maria *et al.*, 1999). Pontine anomalies are reported in the vicinity of the scp, as in the present study, particularly the 'molar tooth sign', in which elongated, thick and mal-orientated scps give the appearance of a molar tooth on axial brain magnetic resonance imaging (Gleeson *et al.*, 2004). Although candidate gene approaches of the Joubert syndrome have failed so far to detect mutation in the WNT1, EN1, EN2 and FGF8 genes of patients (Blair *et al.*, 2002), a link remains possible with the genetic network affected by RA during early development.

The isotretinoin syndrome and various malformations have been described when mothers became pregnant while undergoing skin treatments with oral or topical forms of retinoids (Coberly *et al.*, 1996; Selcen *et al.*, 2000). Moreover, a relationship has been established between the occurrence of birth defects and consumption of vitamin A

at levels close to those recommended during pregnancy (Rothman *et al.*, 1995). Although RA might otherwise have a potential clinical interest to rescue developmental abnormalities at the onset of hindbrain segmentation (Pasqualetti *et al.*, 2001), the present results reinforce the notion that the use of RA should be strictly limited during pregnancy.

Acknowledgements

This work was supported by the European Community (QLG2-CT2001-01467 'Brainstem Genetics'), HFSP (Research Grant 101/97), Ministère de la Recherche (ACI BDP#57), 'RIO Imagerie Gif' plate-form supported by ASTRE, Centre National de la Recherche Scientifique, Fondation pour la Recherche Médicale (FRM) and Ministerio de Ciencia y Tecnología (SAF2002-02731). L.G. was supported by training grants from Fundação para a Ciência e a Tecnologia (PRAXIS XXI, BD/11299/97), Fundação Luso-Americana para o Desenvolvimento (FLAD, Proc. 3.L/A.11/P.281/94) and Embassade de France au Portugal (Convention de Coopération Scientifique, 236 C1). E.D.-d.-T. was supported by The European Community (BIO4-CT975-096) and FRM (EP001227/1) training grants and the Ramón y Cajal's Programme. F.C and L.W. were supported by the French Ministère de l'Education Nationale, de l'Enseignement Supérieur et de la Recherche. We thank the entire Neurobiologie Génétique et Intégrative research unit for valuable discussions and comments during this study.

Abbreviations

AMPA, α-amino-3-hydroxy-5-methyl-4-isoxazolepropionic acid; E, embryonic day; HEB, hyperpnoeic episodic breathing; P, post-natal day; pFRG, parafacial respiratory group; PPTg, pedunculo-pontine tegmental; pre-BötC, pre-Bötzinger complex; r, rhombomere; RA, retinoic acid; scp, superior cerebellar peduncle.

References

Blair, I.P., Gibson, R.R., Bennett, C.L. & Chance, P.F. (2002) Search for genes involved in Joubert syndrome: evidence that one or more major loci are yet to be identified and exclusion of candidate genes EN1, EN2, FGF8 and BARHL1. *Am. J. Med. Genet.*, **107**, 190–196.

Borday, V., Kato, F. & Champagnat, J. (1997) A ventral pontine pathway promotes rhythmic activity in the medulla of neonate mice. *Neuroreport*, **8**, 3679–3683.

Borday, C., Coutinho, A., Germon, I., Champagnat, J. & Fortin, G. (2006) Pre-/post-otic rhombomeric interactions control the emergence of a fetal-like respiratory rhythm in the mouse embryo. *J. Neurobiol.*, **66**, 1285–1301.

Bruce, E.N. & Daubenspeck, J.A. (1995) Mechanisms and analysis of ventilatory stability. In Dempsey, J.A. & Pack, A.I. (Eds), *Regulation of Breathing*. Marcel Dekker, Inc., New York, pp. 285–313.

Chatonnet, F., Domínguez del Toro, E., Voiculescu, O., Charnay, P. & Champagnat, J. (2002) Different respiratory control systems are affected in homozygous and heterozygous kreisler mutant mice. *Eur. J. Neurosci.*, **15**, 684–692.

Chatonnet, F., Boudinot, E., Chatonnet, A., Taysse, L., Daulon, S., Champagnat, J. & Foutz, A.S. (2003a) Respiratory survival mechanisms in acetylcholinesterase knockout mouse. *Eur. J. Neurosci.*, **18**, 1419–1427.

Chatonnet, F., Domínguez del Toro, E., Thoby-Brisson, M., Champagnat, J., Fortin, G., Rijli, F.M. & Thaeron-Antono, C. (2003b) From hindbrain segmentation to breathing after birth: developmental patterning in rhombomeres 3 and 4. *Mol. Neurobiol.*, **28**, 277–294.

Cherniack, N.S. (1999) Apnea and periodic breathing during sleep. *N. Engl. J. Med.*, **341**, 985–987.

Cherniack, N.S., Longobardo, G.S., Levine, O.R., Mellins, R. & Fishman, A.P. (1966) Periodic breathing in dogs. *J. Appl. Physiol.*, **21**, 1847–1854.

Coberly, S., Lammer, E.J. & Alashari, M. (1996) Retinoic acid embryopathy: case report and review of literature. *Pediatr. Pathol. Lab. Med.*, **16**, 823–836.

Conlon, R.A. & Rossant, J. (1992) Exogenous retinoic acid rapidly induces anterior ectopic expression of murine *Hox-2* genes in vivo. *Development*, **116**, 357–368.

Coutinho, A.P., Borday, C., Gilthorpe, J., Jungbluth, S., Champagnat, J., Lumsden, A. & Fortin, G. (2004) Induction of a parafacial rhythm generator by rhombomere 3 in the chick embryo. *J. Neurosci.*, **24**, 9383–9390.

Domínguez del Toro, E., Borday, V., Davenne, M., Neun, R., Rijli, F.M. & Champagnat, J. (2001) Generation of a novel functional neuronal circuit in *Hoxa1* mutant mice. *J. Neurosci.*, **21**, 5637–5642.

Feldman, J.L. & Del Negro, C.A. (2006) Looking for inspiration: new perspectives on respiratory rhythm. *Nat. Rev. Neurosci.*, **7**, 232–242.

Ferland, R.J., Eyaid, W., Collura, R.V., Tully, L.D., Hill, R.S., Al-Nouri, D., Al-Rumayyan, A., Topcu, M., Gascon, G., Bodell, A., Shugart, Y.Y., Ruvolo, M. & Walsh, C.A. (2004) Abnormal cerebellar development and axonal decussation due to mutations in AHI1 in Joubert syndrome. *Nat. Genet.*, **36**, 1008–1013.

Gavalas, A. (2002) ArRAnging the hindbrain. *Trends Neurosci.*, **25**, 61–64.

Giudicelli, F., Taillebourg, E., Charnay, P. & Gilardi-Hebenstreit, P. (2001) Krox-20 patterns the hindbrain through both cell-autonomous and non cell-autonomous mechanisms. *Genes Dev.*, **15**, 567–580.

Gleeson, J.G., Keeler, L.C., Parisi, M.A., Marsh, S.E., Chance, P.F., Glass, I.A., Graham, J.M. Jr, Maria, B.L., Barkovich, A.J. & Dobyns, W.B. (2004) Molar tooth sign of the midbrain-hindbrain junction: occurrence in multiple distinct syndromes. *Am. J. Med. Genet.*, **125A**, 125–134.

Han, F., Subramanian, S., Price, E.R., Nadeau, J. & Strohl, K.P. (2002) Periodic breathing in the mouse. *J. Appl. Physiol.*, **92**, 1133–1140.

Harvey, W.R. (1985) *User's Guide for LSMLMW. Mixed Model Least-Squares and Maximum Likelihood Program*. Ohio University, OH.

Holzschuh, J., Barrallo-Gimeno, A., Ettl, A.K., Durr, K., Knapik, E.W. & Driever, W. (2003) Noradrenergic neurons in the zebrafish hindbrain are induced by retinoic acid and require tfap2a for expression of the neurotransmitter phenotype. *Development*, **130**, 5741–5754.

Jacquin, T.D., Borday, V., Schneider-Maunoury, S., Topilko, P., Ghilini, G., Kato, F., Charnay, P. & Champagnat, J. (1996) Reorganisation of pontine rhythmogenic neuronal networks in *Krox-20* knockout mice. *Neuron*, **17**, 747–758.

Joubert, M., Eisenring, J.J., Robb, J.P. & Andermann, F. (1969) Familial agenesis of the cerebellar vermis. A syndrome of episodic hyperpnoea, abnormal eye movements, ataxia, and retardation. *Neurology*, **19**, 813–825.

Khoo, M.C., Kronauer, R.E., Strohl, K.P. & Slutsky, A.S. (1982) Factors inducing periodic breathing in humans: a general model. *J. Appl. Physiol.*, **53**, 644–659.

Kobayashi, S., Onimaru, H., Inoue, M., Inoue, T. & Sasa, R. (2005) Localization and properties of respiratory neurons in the rostral pons of the newborn rat. *Neuroscience*, **134**, 317–325.

Lagier-Tourenne, C., Boltshauser, E., Breivik, N., Gribaa, M., Betard, C., Barbot, C. & Koenig, M. (2004) Homozygosity mapping of a third Joubert syndrome locus to 6q23. *J. Med. Genet.*, **41**, 273–277.

Li, J.Y.H. & Joyner, A.L. (2001) Otx2 and Gbx2 are required for refinement and not induction of midhindbrain gene expression. *Development*, **128**, 4979–4991.

Lumsden, T.L. (1923) Observation on the respiratory centres in the cat. *J. Physiol.*, **57**, 153–160.

Lumsden, A. & Krumlauf, R. (1996) Patterning the vertebrate neuraxis. *Science*, **274**, 1109–1115.

Maden, M. (2002) Retinoid signalling in the development of the central nervous system. *Nat. Rev. Neurosci.*, **3**, 843–853.

Maria, B.L., Boltshauser, E., Palmer, S. & Tran, T.X. (1999) Clinical features and revised diagnostic criteria in Joubert syndrome. *J. Child. Neurol.*, **14**, 583–590.

Marshall, H., Nonchev, S., Sham, M.H., Muchamore, I., Lumsden, A. & Krumlauf, R. (1992) Retinoic acid alters hindbrain *Hox* code and induces transformation of rhombomeres 2/3 into a 4/5 identity. *Nature*, **360**, 737–741.

McCrimmon, D.R., Milsom, W.K. & Alheid, G.F. (2004) The rhombencephalon and breathing: a view from the pons. *Resp. Physiol. Neurobiol.*, **143**, 103–337.

Mic, F.A., Molotkov, A., Benbrook, D.M. & Duester, G. (2003) Retinoid activation of retinoic acid receptor but not retinoid X receptor is sufficient to rescue lethal defect in retinoic acid synthesis. *P.N.A.S.*, **100**, 7135–7140.

Mitzner, W. & Tankersley, C. (1998) Non invasive measurement of airway responsiveness in allergic mice using barometric plethysmography. *Am. J. Respir. Critic. Care Med.*, **158**, 340.

Mortola, J.P. & Frappell, P.B. (1998) On the barometric method for measurements of ventilation, and its use in small animals. *Can. J. Physiol. Pharmacol.*, **76**, 937–944.

Oury, F., Murakami, Y., Renaud, J.S., Pasqualetti, M., Charnay, P., Ren, S.Y. & Rijli, F.M. (2006) *Hoxa2*- and rhombomere-dependent development of the mouse facial somatosensory map. *Science*, **313**, 1408–1413.

Pasqualetti, M., Neun, R., Davenne, M. & Rijli, F.M. (2001) Retinoic acid rescues inner ear defects in *Hoxa1* deficient mice. *Nat. Genet.*, **29**, 34–39.
Potts, J.T., Rybak, I.A. & Paton, J.F. (2005) Respiratory rhythm entrainment by somatic afferent stimulation. *J. Neurosci.*, **25**, 1965–1978.
Rothman, K.J., Moore, L.L., Singer, M.R., Nguyen, U.S., Mannino, S. & Milunski, A. (1995) Teratogenicity of high vitamin A intake. *N. Eng. J. Med.*, **333**, 1369–1373.
Saraiva, J.M. & Baraitser, M. (1992) Joubert syndrome: a review. *Am. J. Med. Genet.*, **43**, 726–731.
Searle, S.R. (1971) *Linear Models*. John Wiley & Sons, New York.
Selcen, D., Seidman, S. & Nigro, M.A. (2000) Otocerebral anomalies associated with topical tretinoin use. *Brain Dev.*, **22**, 218–220.
Sirbu, I.O., Gresh, L., Barra, J. & Duester, G. (2005) Shifting boundaries of retinoic acid activity control hindbrain segmental gene expression. *Development*, **132**, 2611–2622.
Telgkamp, P., Cao, Y.Q., Basbaum, A.I. & Ramirez, J.-M. (2002) Long-term deprivation of substance P in PPT-A mutant mice alters the anoxic response of the isolated respiratory network. *J. Neurophysiol.*, **88**, 206–213.
Topor, Z.L., Vasilakos, K., Younes, M. & Remmers, J.E. (2007) Model based analysis of sleep disordered breathing in congestive heart failure. *Respir. Physiol. Neurobiol.*, **155**, 82–92.
Wilkinson, D. & Nieto, A. (1993) Detection of messenger RNA by *in situ* hybridization to tissue sections and whole mounts. *Methods Enzymol.*, **225**, 361–373.
Wilkinson, M.H., Berger, P.J., Blanch, N., Brodecky, V. & Jones, C.A. (1997) Paradoxical effect of oxygen administration on breathing stability following post-hyperventilation apnoea in lambs. *J. Physiol. (Lond.)*, **504**, 199–209.
Yamamoto, M., Zhang, J., Smith, D., Hayakawa, Y. & McCaffery, P. (2003) A critical period for retinoic acid teratogenesis and loss of neurophilic migration of pontine nuclei neurons. *Mech. Dev.*, **120**, 701–709.